Biomolecular NMR Assignments
https://doi.org/10.1007/s12104-017-9792-1

ARTICLE

Chemical shift assignments of the partially deuterated Fyn SH2–SH3 domain

Fabien Kieken[1,2,3] · Karine Loth[4,5] · Nico van Nuland[1,2] · Peter Tompa[1,2] · Tom Lenaerts[3,6,7]

Received: 3 July 2017 / Accepted: 28 November 2017

Abstract

Src Homology 2 and 3 (SH2 and SH3) are two key protein interaction modules involved in regulating the activity of many proteins such as tyrosine kinases and phosphatases by respective recognition of phosphotyrosine and proline-rich regions. In the Src family kinases, the inactive state of the protein is the direct result of the interaction of the SH2 and the SH3 domain with intra-molecular regions, leading to a closed structure incompetent with substrate modification. Here, we report the ^{1}H, ^{15}N and ^{13}C backbone- and side-chain chemical shift assignments of the partially deuterated Fyn SH3–SH2 domain and structural differences between tandem and single domains. The BMRB accession number is 27165.

Keywords SH3–SH2 · Tandem domains · NMR · Fyn kinase · Src family

Biological context

The Src family consists of 11 non-receptor tyrosine kinases involved in a plethora of fundamental biological processes including cell growth, differentiation, cellular adhesion, cell migration (Manning et al. 2002). The structural organization of each family member is equivalent: They are composed of four different domains—SH1 to SH4—with a C-terminal negative regulatory tail. The SH4 domain located in the N-terminus anchors the proteins to the plasma membrane and is attributed with the varying physiological functions of the family members (Sato et al. 2009). SH3 and SH2 domains are involved in regulating kinase activity and mediate the interaction of the kinase with its protein partners, and SH1 is the kinase domain (Boggon and Eck 2004; Sicheri and Kuriyan 1997). Src family kinases (SFK) catalytic activity is determined by intermolecular interactions and equilibrium of phosphorylation-dephosphorylation states. Activation of the kinase is triggered by the dephosphorylation of the phospho-tyrosine in the C-terminus, which in turn results in the initiation of signaling cascades that drive basic cellular function (Huculeci et al. 2016; Xu et al. 1999). Given their important role in fundamental physiological and pathological processes, members of the SFK have been widely investigated in various biological contexts.

Fyn, one of the SFK members, regulates numerous cellular processes including motility, growth, differentiation and signal transduction in various cell types (Saito et al. 2010). The Fyn gene has three splice variants, one of which is deemed inactive. FynT is highly expressed in cells of hematopoietic lineage and regulates immune cell functions and inflammatory responses. The other active form FynB is ubiquitous, with the highest expression in the synaptic architecture of the central nervous system, playing important roles in glutamate receptor trafficking and synaptic

✉ Tom Lenaerts
Tom.Lenaerts@ulb.ac.be

[1] Structural Biology Brussels, Vrije Universiteit Brussel, Pleinlaan 2, 1050 Brussel, Belgium

[2] Center for Structural Biology, VIB, Pleinlaan 2, 1050 Brussel, Belgium

[3] AI-lab, Vakgroep Computerwetenschappen, Vrije Universiteit Brussel, Pleinlaan 2, 1050 Brussels, Belgium

[4] Centre de Biophysique Moléculaire, Centre National de la Recherche Scientifique (CNRS) UPR 4301, Université d'Orléans, rue Charles Sadron, 45071 Orléans Cedex 2, France

[5] Collegium Sciences et Techniques, Université d'Orléans, rue de Chartres, 45100 Orléans, France

[6] MLG, Département d'Informatique, Université Libre de Bruxelles, Boulevard du Triomphe, CP 212, 1050 Brussels, Belgium

[7] Interuniversity Institute of Bioinformatics Brussels (IB2), ULB-VUB, La Plaine Campus, Boulevard du Triomphe, CP 263, 1050 Brussels, Belgium

plasticity (Grant et al. 1992; Kojima et al. 1998; Nakazawa et al. 2001; Prybylowski et al. 2005; Suzuki and Okumura-Noji 1995). Beyond it's basic physiological functions, Fyn has been widely investigated as a therapeutic target due to its implication in the pathophysiology of various cancers, neurodegenerative and psychiatric diseases (Nygaard et al. 2014; Ohnuma et al. 2003; Panicker et al. 2015). Fyn has been found significantly upregulated in cancer tissues, with its level correlating with aggressive disease progression and metastasis [review (Elias and Ditzel 2015)], which results from promoting cancer cell proliferation and inhibition of cell death (Elias et al. 2015; Li et al. 2003). Inhibition of Fyn function is thought to have therapeutic potential in cancer and neurodegenerative conditions. Various inhibitors of Fyn kinase domain are available; however these carry various safety liabilities and long term toxicity due to lack of specificity in inhibiting kinase functions (Grant 2009).

Fyn's SH1 activity is regulated by the intramolecular interactions with two of its domains, SH3 and SH2. SH3 domains interact primarily with sequences rich in proline, such as PxxP motifs, although they can also bind other sequences that deviate from the canonical one [review (Saksela and Permi 2012)], whereas SH2 domains recognize and bind phosphotyrosine residues (Pawson 1995). Fyn SH2 is responsible for the state of activation of the kinase. Phosphorylated Tyr527 allows a direct interaction between Fyn SH2 with the C-terminus, resulting in an inactive kinase state. The kinase self-activation occurs during the dephosphorylation of Tyr527 and/or the binding of protein partners, allowing the dissociation between SH3, SH2, and the kinase domain [review in (Roskoski 2015)].

The mechanism of propagation of the information or cross-communication between the two domains is not well investigated and has led to controversial reports. While the SH3 domain enhances Fyn SH2-mediated ligand binding (Panchamoorthy et al. 1994) and the replacement of the SH3–SH2 linker residues with glycines activates c-Src (Young et al. 2001), the analysis of the dynamics of Fyn SH3–SH2 by nuclear magnetic resonance (NMR) T_1/T_2/NOE, domain alignment by residual dipolar couplings and crystallographic structure showed very little structural modifications (Ulmer et al. 2002). Nonetheless, recent work showed that sidechain dynamics plays a role in the activation process (Huculeci et al. 2016).

As no solution structure by NMR of human wild type Fyn SH3–SH2 is available, we report here on the full backbone and side-chain ^{1}H, ^{15}N and ^{13}C assignment of partially deuterated ^{13}C, ^{15}N-labeled Fyn SH3–SH2 in its free form using high-resolution NMR techniques. The anticipated structural resolution of the tandem domains by NMR will provide additional information on changes of structure and dynamics between domains, hopefully providing an explanation for the mechanism of information propagation throughout the structure.

Methods and experiments

Protein expression and purification

The human Fyn SH3–SH2 domain (residues 82–248), SH3 domain (82–147) and SH2 domain (148–248) were subcloned into a pet15b (Novagen) vector containing a thrombin-cleavable N-terminal hexa-His tag by standard cloning methods.

Transformed BL21(DE3)star cells (Invitrogen) were grown at 37 °C in 1 L of minimal medium implemented with 0.75 g $^{15}NH_4Cl$ and 2 g ^{13}C-glucose (Cambridge Isotope Laboratories). The bacteria were induced at a cell density of 0.6 by addition of 0.5 mM IPTG and were then incubated at 22 °C overnight. The cells were pelleted by centrifugation at 7000×*g* and the pellet kept and stored at − 80 °C for further processing. The expression of the partially deuterated and uniformly $^{13}C/^{15}N$-labeled protein was achieved by making the minimal medium 60% in D_2O (Cortecnet) complemented with 0.75 g $^{15}NH_4Cl$ and 2 g ^{13}C-glucose.

The pellets were thawn and resuspended in lysis buffer (20 mM Hepes pH 7.6, 100 mM Na_2SO_4, 20 mM imidazole, 10 mM β-mercaptoethanol (BME), 10% glycerol containing 0.2 mM 4-(2-aminoethyl) benzenesulfonyl fluoride hydrochloride (AEBSF), 5 µg/mL leupeptin and 4 units/mL of DNAse I). The cells were lysed by sonication using a Sonics Vibra-CellTM CV18 model ultrasonic processor (70% amplitude, 3 s pulse on/off for 10 min) and the lysates were centrifuged at 20,000×*g* for 1 h at room temperature. The supernatant was then loaded into a prepacked HisTrap column (GE Healthcare). The resin was washed with 10 column volume of lysis buffer without protease inhibitor and DNAse. The proteins were eluted with 20 mM Hepes pH 7.6, 100 mM Na_2SO_4, 500 mM imidazole, 10 mM BME and 10% glycerol. The eluted proteins were loaded into a gel filtration Econo-Pac 10DG column (Biorad) equilibrated with 20 mM Hepes buffer pH 7.6, 100 mM Na_2SO_4, 10 mM BME, 10% glycerol. The protein were eluted using the same buffer and were concentrated by using 20 mL spinning Vivaspin 20 filters with a 10 kDa cut-off (Sartorius AG) to a concentration of 10 mg/mL. The proteins were either snap frozen and stored at − 80 °C or incubated with 1 unit of thrombin (Calbiochem) per mg of protein overnight at room temperature to remove the His-tag. The cleaved Fyn SH3–SH2 was separated from the tag by gel-filtration using a Superdex75 16/90 column (GE Healthcare) in 50 mM sodium phosphate buffer pH 6.5, 100 mM Na_2SO_4, 2 mM BME. The fractions containing the protein were concentrated using a Vivaspin 20 filter with a 10 kDa

Journal : Large 12104 | Article No : 9792 | Pages : 6 | MS Code : BNMR-D-17-00036 | Dispatch : 28-11-2017

cut-off (Sartorius AG). SDS-PAGE was used to determine the purity of the sample.

NMR spectroscopy

The concentration of partially deuterated $^{15}N/^{13}C$ sample of Fyn SH3–SH2 used for assignment was 0.7 mM in 50 mM sodium phosphate buffer pH 6.5, 100 mM Na_2SO_4, 2 mM BME, 10% D_2O. NMR data were acquired at 25 °C on a Varian Direct-Drive System 600 MHz and an Avance III HD Bruker 700 MHz spectrometers, both equipped with a cryoprobe. Sequential assignments of the protein were carried out using ^{15}N-HSQC, ^{13}C-HSQC, HNCO, HNCA, HNCACB, following classical procedures Side-chains assignments were carried out using trosy-HBHANH, trosy-HBHA(CO)NH, HCCH-TOCSY, [^1H,^{15}N]-HSQC NOESY and [^1H,^{13}C]-HSQC NOESY. Backbone assignments were obtained using 2D 15N-HSQC, 13C-HSQC, 3D ^{15}N and ^{13}C NOESY-HSQC (mixing time: 100 ms) and triple-resonance experiments CBCACONH, HNCACB, HCCH-TOCSY, HBHANH, HBHACONH. 1D ^1H-detected ^{15}N-edited relaxation experiments were used to calculate the average ^{15}N T_1 and T_2 relaxation by fitting the integrated signal in the backbone amide ^1H region of the spectrum (10.5–8.5 ppm) as a function of delay time to an exponential decay. ^{15}N T_1 and T_2 spectra were acquired with a recycle delay of 8.0 s. T_1 relaxation delays of 100, 200, 300, 400, 600, 800, 1000, 1500, 2000, 3000 and 5000 ms and T_2 relaxation delays of 10, 30, 50, 70, 90, 110, 130, 150, 170 ms were used for data collection. At high magnetic field (above 500 MHz), the correlation time of a molecule (τ_C) can be estimated for a rigid protein with $\tau_C >> 0.5$ ns as a function of the ratio of the longitudinal (T_1) and transverse (T_2) ^{15}N relaxation times. By considering J(0) and J(ω_N) spectral density terms and neglecting higher frequency terms, the correlation time of a molecule can be estimated using the following equation:

$$\tau_C \approx \frac{1}{4\pi\nu_N}\sqrt{6\frac{T_1}{T_2} - 7},$$

where ν_N is the ^{15}N resonance frequency (in Hz) (Kay et al. 1989).

All 3D experiments were acquired using non-uniform sampling. All NMR spectra were processed using NMRPipe (Delaglio et al. 1995) or Bruker's Topspin 3.2™ and analysed by NMRVIEW and CCPNMR (Johnson and Blevins 1994; Vranken et al. 2005).

Assignment and data deposition

Analysis of Fyn SH3–SH2 domain 1D ^1H-detected ^{15}N-edited relaxation experiments in solution showed a direct relation between the protein correlation time (τ_C) with its concentration, suggesting that the protein under the conditions of the NMR experiments is a monomer–dimer mixture (Fig. 1a) (Rossi et al. 2010). The correlation time of a monomeric protein in solution in nanoseconds is approximately 0.6 times its molecular weight in kDa. For Fyn SH3–SH2, τ_C is estimated to be 11.8 ns. At classical sample concentration for NMR structure determination (> 0.6 mM), the τ_c for Fyn SH3–SH2 is above 16.5 ns. The quality of HSQC spectra decreases with incremental concentrations (Fig. 1b) and as a consequence, use of uniformly-labeled $^{15}N/^{13}C$ sample yielded no signal in all 3D experiments (Fig. 1c).

Nietlispach et al. showed that 50–60% random fractional deuteration increases the sensitivity of the NMR experiments due to the reduction of R_2 of the molecule, allowing structure determination by NMR using ^{15}N and ^{13}C NOESY-HSQC (Nietlispach et al. 1996). Using this methodology on the Fyn SH3–SH2 domain, we observed a significant improvement on the quality of the NMR spectra (Fig. 1d). Using this approach with a 50% deuterated uniformly-labeled ^{15}N and ^{13}C Fyn SH3–SH2 resulted in 97% of the backbone and 94% of all ^1H side chains assignment. Due to the random nature of the deuteration processes, the chemical shifts were not corrected for ^2H isotopes shifts. The ^{15}N-HSQC spectrum and assignment are displayed in Fig. 2a. The ^1H, ^{13}C and ^{15}N chemical shifts were deposited into the BioMagResBank database (http://www.brmb.wisc.edu/) accession number 27165.

To determine the percentage of monomer/dimer complexes, we performed an analysis of 1D ^{15}N T_1/T_2 at 50–2000 µM concentrations (Fig. 1a). The estimated K_D was calculated at 500 and 600 mM, suggesting that more than 60% of Fyn SH2–SH3 exists as a dimer at 0.7 mM. For maintenance of dominant monomeric FYN—SH3–SH2 in solution, lower concentrations (0.1–0.2 mM) are necessary; however, such experimental prerequisites hinder spectral assignment and structure determination due to lack of signal.

Increasing sample concentrations above 1 mM also resulted in loss of NMR signal (broadened peaks; Fig. 1b). Dimer formation favoured by higher sample concentrations exhibited as broadened peaks with the exception of one peak (R96), which slightly shifted without creating ambiguity for its assignment. Analysis of this chemical shift perturbation enabled K_D determination in the range of 500–700 mM. Thus a concentration of 0.7 mM was subsequently selected for all the experiments in this study.

Journal : Large 12104 | Article No : 9792 | Pages : 6 | MS Code : BNMR-D-17-00036 | Dispatch : 28-11-2017

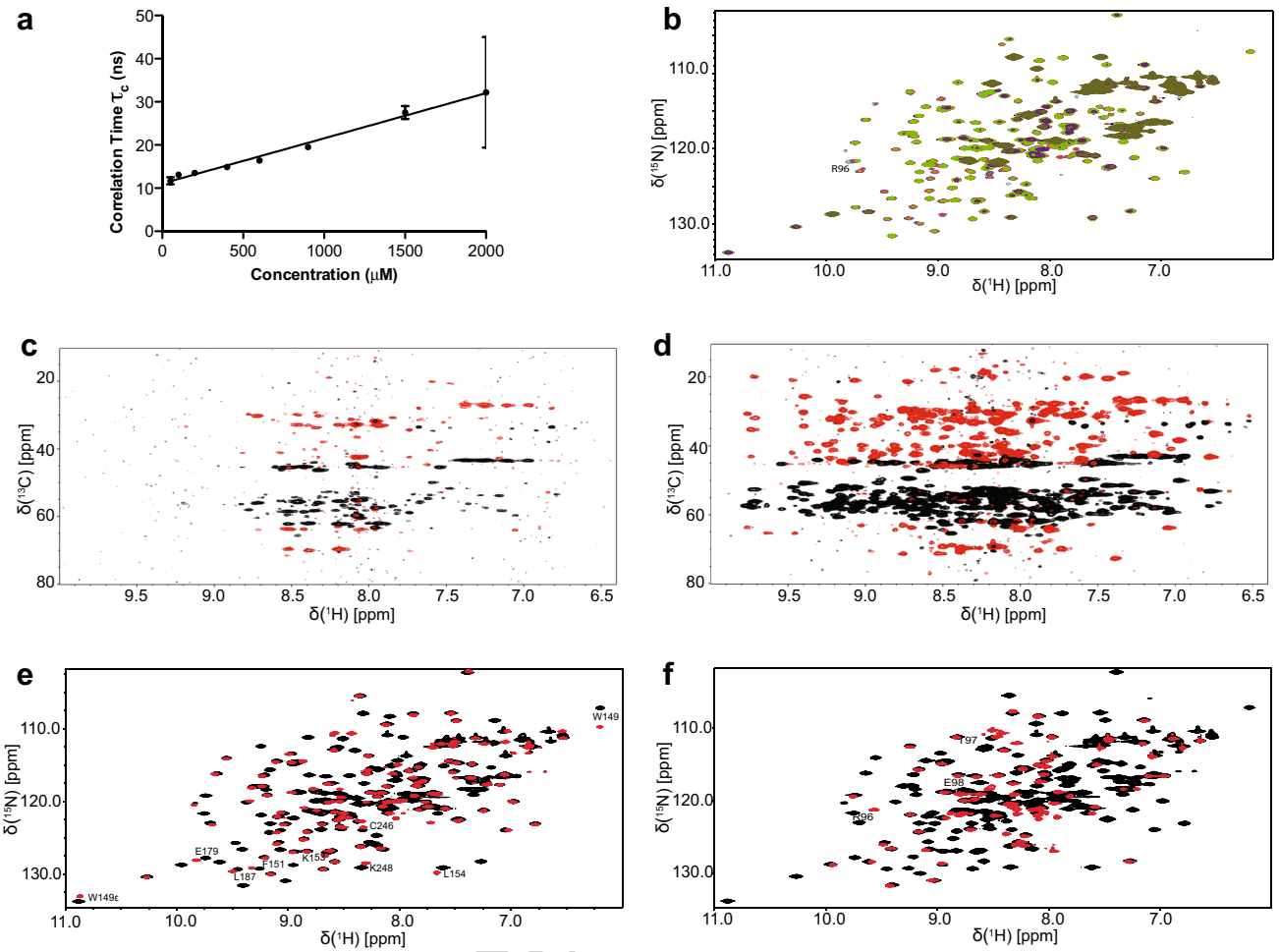

Fig. 1 Effect of protein concentration and deuteration on the NMR experiment and structural differences between Fyn SH3–SH2 and Fyn single domains SH2 and SH3. Plot of Fyn SH2–SH3 correlation time (τ_C) in function of protein concentration (**a**). Overlay of ^{15}N-HSQCs of the Fyn SH3–SH2 domain collected at different protein concentrations (**b**) (black: 50 μM; gray: 100 μM; light blue: 200 μM; dark blue: 400 μM; red: 600 μM; green: 900 μ; purple: 1.5 mM and dark green: 2 mM). 2D ^{1}H/^{13}C projection of the 3D HNCACB for a deuteration level of 0% (**c**) and 50% (**d**). ^{15}N-HSQC overlay spectra of Fyn SH3–SH2 domain (black) in the presence of the His tagged Fyn SH2 (**e**) and SH3 (**f**) domains (red). Residues affected by the presence of the tandem domains have been labeled

The chemical shift index (CSI) function and DANGLE (Cheung et al. 2010) modules in CCPNMR were used to predict the secondary structure of Fyn SH3–SH2 from backbone chemical shifts (Fig. 2b). The predicted secondary structure is an arrangement of 6 β-strands for the SH3 domain and 5 β-strands and 2 α-helices for SH2 domain, with a short α-helix in the linker between the two domains. These data further corroborate previous reports on the structure of SH2 and SH3, as a β-sandwich consisting of six strands flanked by 2 α-helices and connected by three loops and a β-sandwich consisting of five strands flanked by three loops and a short 3_{10} helix, respectively (Xu et al. 1999).

The structure of Fyn SH2 free in solution and in complex with the phosphorylated tail of the protein has been solved recently (Huculeci et al. 2016). We compared the ^{15}N HSQC spectrum of the SH3–SH2 domain with the single SH2 domain under identical conditions to investigate if there is an effect of the SH3 domain on the structure of SH2 domain. We observed the expected changes in the N-terminal region, but also throughout the sequence (Fig. 1e) suggesting a change in the structure of the SH2 domain when linked to the SH3 domain. A similar experiment using the free SH3 domain resulted in similar changes in the SH2 domain, with some still present, especially in the loop area between b1 et b2 (Fig. 1f). These data underline the importance of studying these domains within the context of the tandem SH2–SH3 domain or even the full-length protein, as these differences may have an impact on the potential sidechain-induced communication between different parts of a protein.

Journal : Large 12104 | Article No : 9792 | Pages : 6 | MS Code : BNMR-D-17-00036 | Dispatch : 28-11-2017

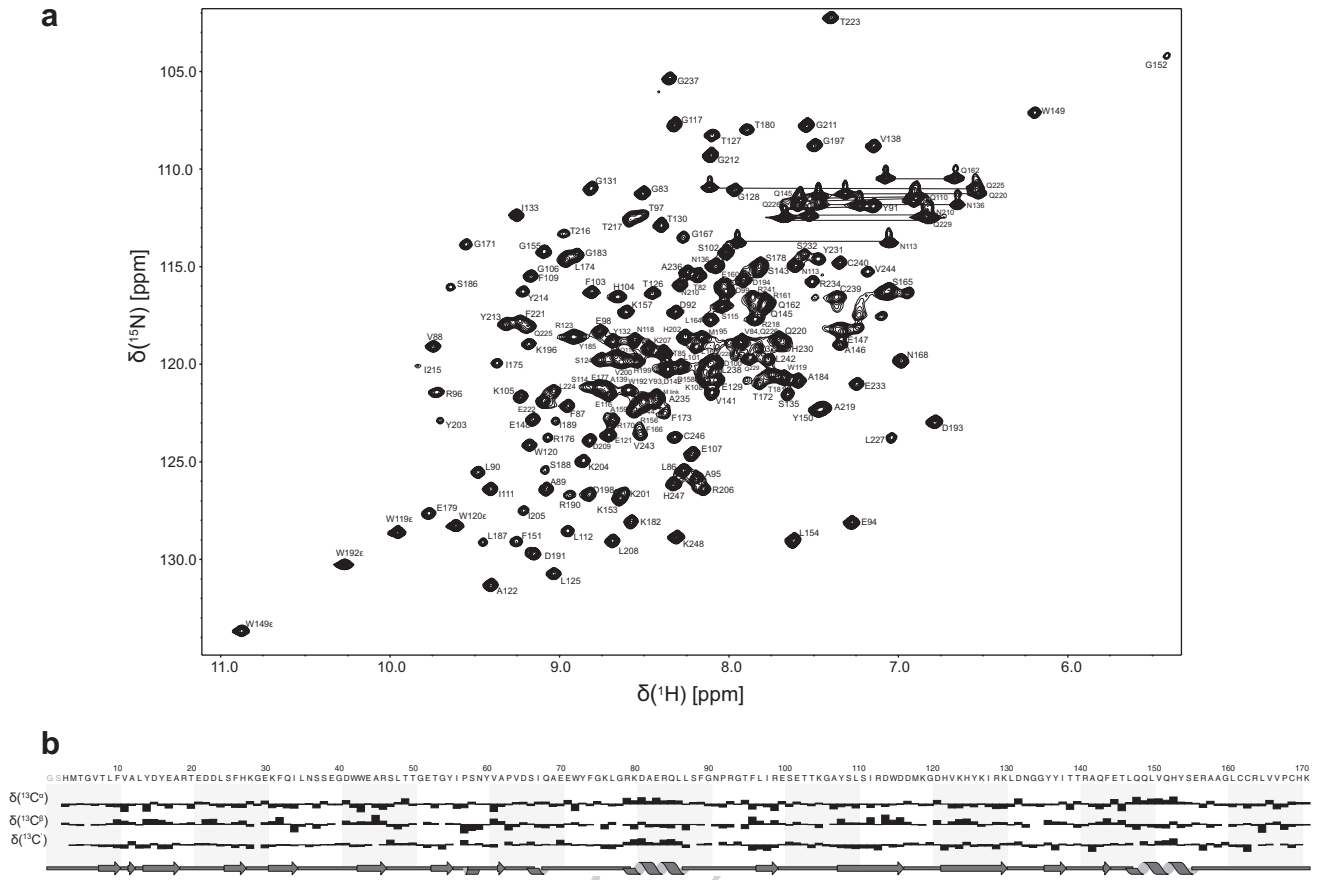

Fig. 2 Assigned ^{15}N-HSQC spectrum and secondary structure prediction of the Fyn SH3–SH2 domain. **a** ^{15}N-HSQC spectrum of Fyn SH3–SH2 domain in 50 mM sodium phosphate buffer pH 6.5, 100 mM Na_2SO_4, 2 mM BME, 10% D_2O. The assignments of backbone side chain amides and tryptophan indole groups are labeled. **b** Threshold deviation from random coil ^{13}CO, ^{13}Cα and ^{13}Cβ were plotted as a function of residue number using the chemical shift index (CSI) module in CCPNMR. The cartoon represents the secondary structure of Fyn SH3–SH2 predicted by the CSI and DANGLE modules in CCPNMR

Acknowledgements This research is funded by the Flemish Scientific Fund (F.W.O.) via the grant G025915N. The VIB and the Jean Jeener NMR Center provided further support for our work.

References

Boggon TJ, Eck MJ (2004) Structure and regulation of Src family kinases. Oncogene 23:7918–7927

Cheung MS, Maguire ML, Stevens TJ, Broadhurst RW (2010) DANGLE: A Bayesian inferential method for predicting protein backbone dihedral angles and secondary structure. J Magn Reson 202:223

Delaglio F, Grzesiek S, Vuister GW, Zhu G, Pfeifer J, Bax A (1995) NMRPipe: a multidimensional spectral processing system based on UNIX pipes. J Biomol NMR 6:277–293

Elias D, Ditzel HJ (2015) Fyn is an important molecule in cancer pathogenesis and drug resistance. Pharmacol Res 100:250–254

Elias D, Vever H, Laenkholm AV, Gjerstorff MF, Yde CW, Lykkesfeldt AE, Ditzel HJ (2015) Gene expression profiling identifies FYN as an important molecule in tamoxifen resistance and a predictor of early recurrence in patients treated with endocrine therapy. Oncogene 34:1919–1927

Grant SK (2009) Therapeutic protein kinase inhibitors. Cell Mol Life Sci 66:1163–1177

Grant SG, O'Dell TJ, Karl KA, Stein PL, Soriano P, Kandel ER (1992) Impaired long-term potentiation, spatial learning, and hippocampal development in fyn mutant mice. Science 258:1903–1910

Huculeci R et al (2016) Dynamically coupled residues within the SH2 domain of Fyn are key to unlocking its activity. Structure 24:1947–1959

Johnson BA, Blevins RA (1994) NMR view: a computer program for the visualization and analysis of NMR data. J Biomol NMR 4:603–614

Kay LE, Torchia DA, Bax A (1989) Backbone dynamics of proteins as studied by 15N inverse detected heteronuclear NMR spectroscopy: application to staphylococcal nuclease. Biochemistry 28:8972–8979

Kojima N, Ishibashi H, Obata K, Kandel ER (1998) Higher seizure susceptibility and enhanced tyrosine phosphorylation of *N*-methyl-D-aspartate receptor subunit 2B in fyn transgenic mice. Learn Mem 5:429–445

Li X et al (2003) Alphavbeta6-Fyn signaling promotes oral cancer progression. J Biol Chem 278:41646–41653

Manning G, Whyte DB, Martinez R, Hunter T, Sudarsanam S (2002) The protein kinase complement of the human genome. Science 298:1912–1934

Nakazawa T et al (2001) Characterization of Fyn-mediated tyrosine phosphorylation sites on GluR epsilon 2 (NR2B) subunit of the *N*-methyl-D-aspartate receptor. J Biol Chem 276:693–699

Nietlispach D et al (1996) An approach to the structure determination of larger proteins using triple resonance nmr experiments in conjunction with random fractional deuteration. J Am Chem Soc 118:407–415

Nygaard HB, van Dyck CH, Strittmatter SM (2014) Fyn kinase inhibition as a novel therapy for Alzheimer's disease. Alzheimers Res Ther 6:8

Ohnuma T, Kato H, Arai H, McKenna PJ, Emson PC (2003) Expression of Fyn, a non-receptor tyrosine kinase in prefrontal cortex from patients with schizophrenia and its correlation with clinical onset. Brain Res Mol Brain Res 112:90–94

Panchamoorthy G et al (1994) Physical and functional interactions between SH2 and SH3 domains of the Src family protein tyrosine kinase p59fyn. Mol Cell Biol 14:6372–6385

Panicker N et al (2015) Fyn kinase regulates microglial neuroinflammatory responses in cell culture and animal models of parkinson's disease. J Neurosci 35:10058–10077

Pawson T (1995) Protein modules and signalling networks. Nature 373:573–580

Prybylowski K, Chang K, Sans N, Kan L, Vicini S, Wenthold RJ (2005) The synaptic localization of NR2B-containing NMDA receptors is controlled by interactions with PDZ proteins and AP-2. Neuron 47:845–857

Roskoski R Jr (2015) Src protein-tyrosine kinase structure, mechanism, and small molecule inhibitors. Pharmacol Res 94:9–25

Rossi P et al (2010) A microscale protein NMR sample screening pipeline. J Biomol NMR 46:11–22

Saito YD, Jensen AR, Salgia R, Posadas EM (2010) Fyn: a novel molecular target in cancer. Cancer 116:1629–1637

Saksela K, Permi P (2012) SH3 domain ligand binding: What's the consensus and where's the specificity? FEBS Lett 586:2609–2614

Sato I et al (2009) Differential trafficking of Src, Lyn, Yes and Fyn is specified by the state of palmitoylation in the SH4 domain. J Cell Sci 122:965–975

Sicheri F, Kuriyan J (1997) Structures of Src-family tyrosine kinases. Curr Opin Struct Biol 7:777–785

Suzuki T, Okumura-Noji K (1995) NMDA receptor subunits epsilon 1 (NR2A) and epsilon 2 (NR2B) are substrates for Fyn in the postsynaptic density fraction isolated from the rat brain. Biochem Biophys Res Commun 216:582–588

Ulmer TS, Werner JM, Campbell ID (2002) SH3-SH2 domain orientation in Src kinases: NMR studies of Fyn. Structure 10:901–911

Vranken WF et al (2005) The CCPN data model for NMR spectroscopy: development of a software pipeline. Proteins 59:687–696

Xu W, Doshi A, Lei M, Eck MJ, Harrison SC (1999) Crystal structures of c-Src reveal features of its autoinhibitory mechanism. Mol Cell 3:629–638

Young MA, Gonfloni S, Superti-Furga G, Roux B, Kuriyan J (2001) Dynamic coupling between the SH2 and SH3 domains of c-Src and Hck underlies their inactivation by C-terminal tyrosine phosphorylation. Cell 105:115–126